THEORETICAL STUDY OF THE ANTIPARALLEL DOUBLE-STRANDED HELICAL DIMER OF GRAMICIDIN AS AN ION CHANNEL

SHEN-SHU SUNG AND PETER C. JORDAN
Department of Chemistry, Brandeis University, Waltham, Massachusetts 02254

ABSTRACT Recent experimental studies by Durkin, J. T., O. S. Andersen, F. Heitz, Y. Trudelle, and R. E. Koeppe II (1987. *Biophys. J.* 51:451*a*) have suggested that the antiparallel double-stranded helical (APDS) dimer of gramicidin can form a transmembrane cation channel. This article reports a theoretical study that successfully rationalizes the channel properties of the APDS dimer. As in the case of the head-to-head (HH) dimer, the APDS exhibits a high potential energy barrier as anions approach the channel mouth, accounting for the observation of valence selectivity. The calculated potential energies of cations show two binding sites near the channel mouths, a typical feature of the HH channel. The potential energies of hydrated cations in the APDS are generally higher than those in the HH channel and show a larger pseudoperiodicity and higher barriers, an observation which suggests that the APDS should exhibit lower single channel conductance.

INTRODUCTION

Gramicidin, a model system for biological channels, has been intensively investigated both experimentally and theoretically. The dominant structure of the transmembrane ionic channel is the head-to-head (HH) dimer, originally proposed by Urry (1, 2). Very recently, the experimental work on hybrid 14-mers of gramicidin C and the optically reversed analogue gramicidin M^- by Durkin et al (3) has suggested that the antiparallel double stranded helix (APDS) dimer, noted as a possible form of gramicidin dimer by Veatch et al. 15 years ago (4), may also serve as a transmembrane ionic channel. It appears to have a much longer lifetime than, and to be essentially as cation selective as the more familiar electrically active form, the HH dimer. Crystallographic evidence (5, 6) indicates that this channel, when crystallized from alcoholic cesium electrolytes, has the same length, 26 Å, and the same pore size, 3.8 Å, as that inferred for the HH dimer. They both have peptide polar groups lining the interior of the helix and hydrophobic sidechains facing outwards toward the membrane. The backbone structure of APDS is shown in Fig. 1 *a*, with that of HH illustrated in Fig. 1 *b* for comparison. The atomic coordinates in Fig. 1 and in all our calculations are obtained from conformational analysis by Koeppe et al. (7). This article reports a theoretical investigation of the channel properties of the APDS dimer of gramicidin.

MODEL AND METHOD

A detailed description of both model and method has been provided in previous publications (8, 9). Here we briefly mention its main features.

In most of our calculations only the polar groups of the gramicidin backbone (the polyglycine analogue) are included for computational economy. Occasionally, the α-carbon atoms are also included in the calculations to confirm a qualitative conclusion or to verify a structural configuration. Each polar group (CO and NH) of the peptide linkage is modeled by a polarizable dipole oscillating about its equilibrium position and tilting about its original orientation. The force constant and the torsional constant are chosen to be 0.5 mdyn/Å and 0.5×10^{-18} J, respectively, corresponding to vibrational frequencies in the range of 200–500 cm^{-1}. The permanent dipole moments of the CO and NH groups determined from their uncompensated partial charges are 2.262 and 0.864 Debye, respectively (10); the polarizabilities of CO and NH groups are 1.82 and 1.44 $Å^3$, respectively (11).

The polarizable electropole model of water (12) is used; water is described as a polarizable sphere with a dipole and a quadrupole located at its center of mass. The permanent dipole moment is 1.855 Debye, the experimental value in gaseous water (13). The quadrupole moments are Q_{xx} = 4.844 DÅ and Q_{yy} = 5.060 DÅ, obtained from quantum mechanical calculation (14), and the polarizability (15) is 1.444 $Å^3$. The ions are charged, polarizable spheres with polarizabilities 2.855 and 2.156 $Å^3$ for Cs^+ and Cl^-, respectively (16). The total dipole moment of the various polarizable moieties is the sum of the permanent dipole moment and an induced dipole moment, assumed to be the product of the electrical field and the isotropic polarizability. The resultant dipole moments are computed by an iterative method until self-consistency is achieved. Thus electronic reorganization is taken into account in this approach. Then the energy, the forces, and the torques are evaluated.

The total energy is the sum of five terms: the electrostatic energy, the polarization energy, the Lennard-Jones energy, the group vibrational energy, and the group torsional energy. The parameters for the 6–12 Lennard-Jones potential describing water–water interaction are 3.149 Å and 0.425 kcal/mol, determined by Gellatly et al. (17) by fitting the water dimer properties. For ion-water interaction the parameters (18) were obtained by fitting the experimental hydration enthalpies (19, 20) and ion-water distances (21).

The potential energies and the structures were calculated by a molecular dynamics program. At each position along the channel axis (defined as the z axis) the ions were allowed to move in the plane perpendicular to the axis to minimize the energy at the given z value. The potential energies and the equilibrium geometries were obtained by cooling down the system

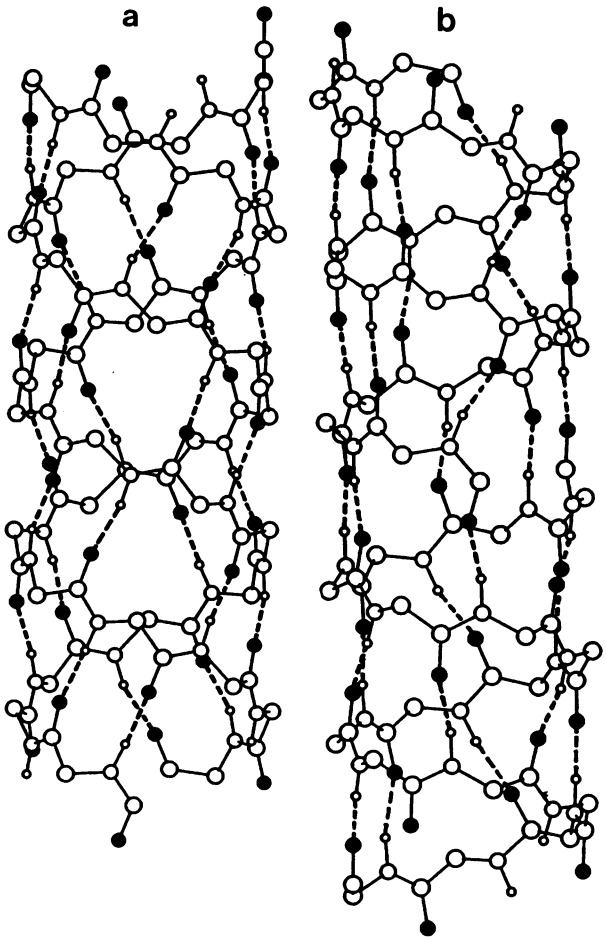

FIGURE 1 The backbone structure of the gramicidin dimers. (*a*) The antiparallel double-stranded helix and (*b*) the head-to-head dimer. (*Small circles*) Hydrogen atoms of the NH groups. (*Solid circles*) Oxygen atoms of the CO groups. (*Dashed lines*) The 28 hydrogen bonds in each dimer.

to 10^{-5} K. Because more than one minimum is possible for each value of z, several initial configurations were tested and the lowest energy obtained was taken as the potential energy at that z. In what follows energy always refers to the potential energy of a static configuration, rather than the free energy of a dynamic system.

Our treatment of channel solvation is highly approximate. Thermal effects, the effect of the membrane and bulk water, the influence of the amino acid side chains and of very low frequency vibrational modes have all been ignored. This study, like our earlier ones (8, 9, 22, 23), focuses on the energetic and structural influence of the polypeptide backbone.

The algorithm proposed by Gear (24) and the Cayley-Klein parameter method of Evans and Murad (25) were used in solving the equations of motion.

EMPTY CHANNEL

With neither ions nor water present the electrostatic interaction and polarization of the peptide groups cause them to relax from their original positions and orientations and reach a polarization equilibrium. For a single strand (the monomer) of the APDS dimer this self-interaction energy is −29.0 kcal/mol; for a monomer of the HH helix the corresponding energy is much lower, −64.6 kcal/mol, mainly due to the presence of 11 intramonomer hydrogen bonds. In the APDS form each strand is twice as long as that of a monomer of HH and cannot form intrastrand hydrogen bonds. All hydrogen bonds are formed between the two strands.

The total interaction energy among the polar groups in the APDS is −129.2 kcal/mol, and the strand–strand binding energy (the dimerization energy) is therefore −71.2 kcal/mol. In HH these are −148.1 kcal/mol and −18.9 kcal/mol, respectively. The much larger dimerization energy of APDS mainly reflects the 28 hydrogen bonds formed between the two strands. In HH there are only six. The experimentally observed long lifetime of the dimer could be attributed to the large dimerization energy in APDS. Including the α-carbons in the calculation also yields a higher total energy and a larger dimerization energy for APDS.

Our calculations indicate a lower total energy for an isolated HH dimer, because in its equilibrium configuration the hydrogen bond distances are ~0.1 Å shorter on average than in APDS. The relative stabilities of the APDS dimer and the HH dimer depend on the environment. The dominant role of the HH dimer as the transmembrane gramicidin channel indicates its stability in the environment of lipid membrane and aqueous solution. The APDS dimer shows its stability in the solid crystallized from the alcoholic cesium electrolytes (5, 6). Besides the crystal packing factor, these ions play an important role in stabilizing this APDS structure. In this crystal form, each unit cell contains two gramicidin dimers, with two Cs^+ and three anions in each dimer and with two Cs^+ between the dimers. When no ions are present, the APDS dimer has a different structure (32 Å long and 2 Å pore radius, 26).

The static and dynamic behavior of ions and water in the channel depends on the electric potential and its derivatives (electric field, etc.) at the locations of the ion and water. Fig. 2, *a* and *b*, show the electric potentials on the helical axis for APDS and HH, respectively. The electric potential unit used in the figures has been converted to kilocalories per mole for monovalent cations, for convenience of comparison with the energy profiles to be described later. The dotted lines in the figures are for each isolated monomer, where the terminus exhibiting the higher potential maximum is the formyl end. The electric potential curve for each monomer in Fig. 2 *a* is essentially an axially elongated form of that of a monomer in Fig. 2 *b*, because each monomer in APDS spans twice the length in the axial direction. In Fig. 2, *a* and *b*, the dimer potential is quite close to being a superposition of the two monomer potentials. The major difference in Fig. 2 *b* is in the central region, where the polarization interaction of the two monomers is significant. In fact, in the HH channel all six intermonomer hydrogen bonds are formed in this region and cause the electric potential of the dimer to be ~6 kcal/mol higher than is the sum of the isolated monomer potentials. It is the dimerization that creates the maximum

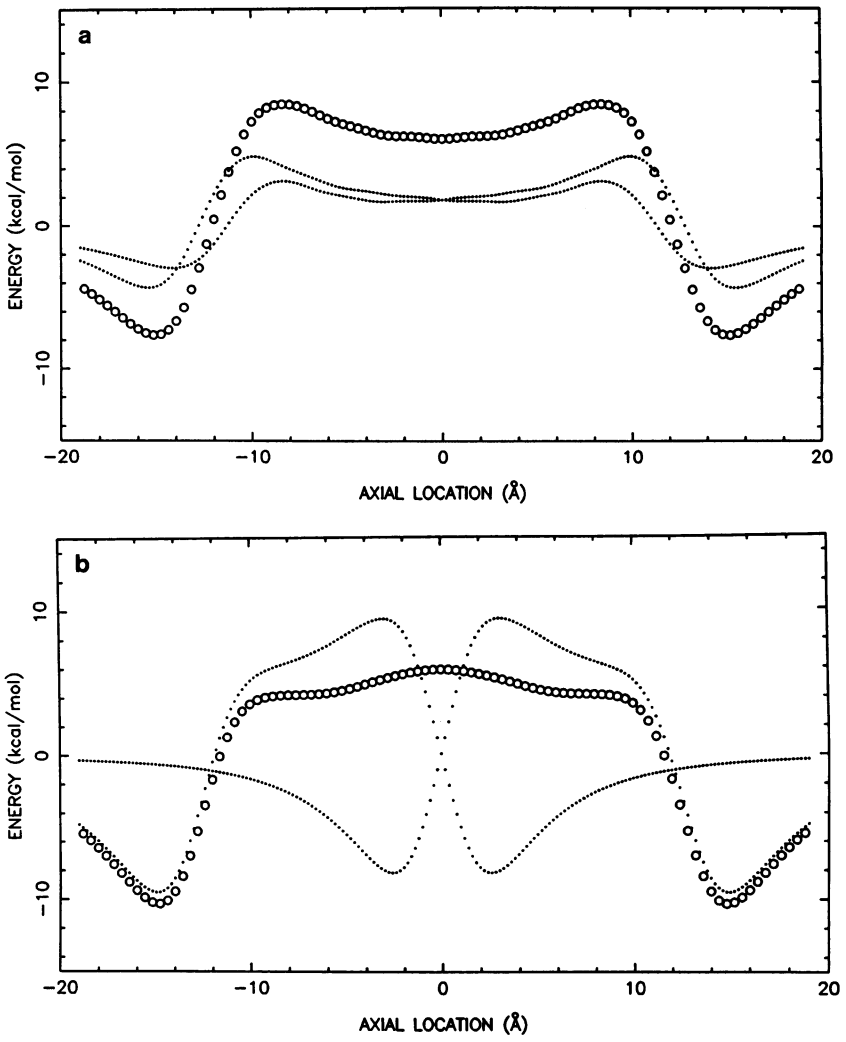

FIGURE 2 (*Circles*) The electric potentials on the helical axes of the two gramicidin dimers. (*a*) APDS and (*b*) HH. Both potentials are negative at the ends and positive in the middle, suggesting the same valence selectivity, but the potential for APDS is higher, suggesting a smaller cation conductance. (*Dotted lines*) Electric potentials due to an isolated strand of APDS or an isolated monomer of HH.

in the center of the potential curve. In Fig. 2 *a* the dimer potential is ~2 kcal/mol higher than the sum of the monomer potentials in the whole region between −9 and 9 Å and ~0.6 kcal/mol lower at −15 and 15 Å. This is because the two monomers interact closely in the whole length of the helix and form 28 hydrogen bonds between the two monomers. Naturally the dimerization changes the charge distribution and electric field of the monomer throughout the whole helix. This is consistent with the large calculated dimerization energy of the APDS channel.

Despite the different monomer–monomer interactions and the different structure, the general shapes of the dimer potentials in Fig. 2, *a* and *b*, have many features in common. Both potentials have minima at ~15 Å from the helix midpoint, suggesting possible cation binding sites near the mouths, and barriers to prevent anions from entering the channel. Both potentials rise steeply in the region from 15 to ~10 Å, and both are relatively flat in the central region of the channel. These common features determine that they are both cation-selective, a point to be discussed in detail later.

The origin of the electric potential is the charge distribution in the channel. The sum of the axial components of the APDS group dipoles is 3.52 Debye in the negative z region and −3.52 Debye in the positive z region. Therefore one may consider the whole channel as an axial quadrupole, which is negative at both ends and positive at its midpoint. This is qualitatively the same as the HH channel (22). After careful comparison of the APDS and the HH dimers we find that the polar groups in the APDS channel are oriented less parallel to the helical axis. Hence, compared with the HH channel, the group dipoles in the APDS channel have slightly smaller axial components and slightly larger radial and tangential (perpendicular to both axial and radial directions) components.

The electric potential of the APDS channel in Fig. 2 *a* ranges from −7.64 kcal/mol (at −15.1 Å) to 8.44 kcal/mol (at −8.3 Å), whereas that of the HH channel in Fig. 2 *b* runs from −10.33 kcal/mol (at 14.9 Å) to 5.88 kcal/mol (at the midpoint). The potential variations are nearly equal (16.08 vs. 16.21 kcal/mol) in both channels. However, the potential in the APDS channel is 2.6 to 2.7 kcal/mol higher due to differences in the radial components of the

group dipoles. For the HH channel the sum of the radial components of the polar groups is positive (1.00 Debye), i.e., pointing outwards; the potential on the channel axis is consequently lower. For the APDS channel this sum is slightly negative (−0.34 Debye), i.e., pointing inwards and the potential on the axis is higher. Therefore, in the APDS channel cation energies should be higher and anion energies should be lower than in the HH channel. This will be discussed in the following section.

The relative energy changes in Fig. 2, *a* and *b*, are also different. The potential increase from 15.1 Å (minimum) to 8.3 Å (maximum) in Fig. 2 *a* is 16.0 kcal/mol, 1.6 kcal/mol higher than that in the corresponding range in Fig. 2 *b*. This could cause a higher barrier in the APDS channel as a cation moves towards the midpoint from the binding sites. From 8.3 Å towards the midpoint the potential slowly decreases and reaches a local minimum at the midpoint in the APDS channel, whereas it increases and reaches its global maximum in the HH channel.

ION-APDS INTERACTION

Naturally, one expects the energy profiles of an ion to mimic the general features of the electric potential of Fig. 2. For an anion the energy profile should be roughly an inverted form of the electric potential, because of the ion's negative charge. However, incorporating an ion changes the polarizations, orientations, and locations of the channel groups, especially for groups close to the ion. Furthermore, the ion is not located on the channel axis, while the electric potentials in Fig. 2 are axial. Therefore the energy profiles of ions in the channel need not conform identically to the electric potential on the channel axis.

Within a certain distance (for example, half the channel length) an ion in the central region interacts with more channel groups than one in the channel end. Therefore, the energy profiles of ions in Fig. 3 show lower energies in the central region, compared with what would be expected from the corresponding electric potential in an empty channel.

At some z coordinates an ion interacts more favorably with the channel groups and is pulled further from the axis than at other z locations. The energy profile therefore shows small wiggles reflecting the pseudoperiodicity of the peptide chain. This is clearly shown in the central region of the Cl^- profile in Fig. 3.

The pseudoperiodicity in the HH channel is 1.5 Å, which is the axial distance between the corresponding CO (or NH) groups of two adjacent dipeptide units. In the APDS channel each strand spans the twice axial length as does a monomer in the HH channel and the pseudoperiodicity for each strand, and consequently that of the dimer (the periodicities of the two strands are neither exactly in phase nor out of phase), is ~3 Å.

However, this periodicity is not reflected in the Cs^+ profile shown in Fig. 3. After examining energy partitioning for Cs^+ at each axial position we found the following

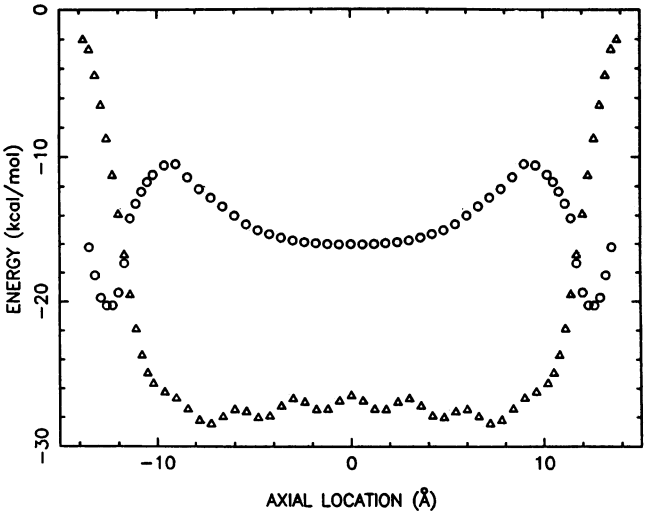

FIGURE 3 Ion-APDS interaction energies with no water present. (*Triangles*) Cl^-. (*Circles*) Cs^+. The potential energy of Cl^- is much higher at the ends, indicating a very large entry barrier. As noted in the text, for Cs^+ there are no perceptible intermediate minima; for Cl^- there are six interior minima.

reason for the lack of structure. The low-energy Cs^+ trajectory is a helix of the same handedness and pitch as that of the channel helix. At each location Cs^+ is usually bound most strongly to two CO groups, one from each strand. As Cs^+ moves along the axis, the CO groups with which it binds most strongly change. The APDS structure happens to be such that when Cs^+ shifts between two CO groups of one strand, it binds most strongly with a CO of the other strand. This causes the local energy fluctuations due to channel pseudoperiodicity to be so small as to be imperceptible. In fact, the energy at the midpoint is 0.02 kcal/mol higher than that at 0.9 Å from the midpoint. When water molecules are included in the calculation, the energy profile in the region between 9.3 and −9.3 Å is no longer structureless.

Before examining Cs^+ interaction with the APDS channel, we compare the energy profiles for Cs^+ and for Cl^- to determine the origin of the valence selectivity. In the mouth region Cl^- energy changes rapidly. At $|z| > 15$ Å the energy is positive (not shown in Fig. 3). At $z = 18$ Å there is an energy barrier of ~2 kcal/mol due to the electric potential wells near each mouth in Fig. 2 *a*. When Cl^- approaches a channel mouth from outside, its interaction with the APDS is repulsive. Because bulk water is not included in these calculations, the relative value compared with Cs^+ is more meaningful than the absolute value for Cl^- itself. At 15 Å the Cl^- energy is ~20 kcal/mol higher (less stable) than that of the similar-sized cation Cs^+, suggesting a conductance 10^{10} times less than for Cs^+. In other words, the APDS channel should be practically impermeable to Cl^-. This is consistent with the experimental observation on the proposed APDS channel (3). The very low energy of Cl^- inside may be related to its stability inside the crystalline APDS (6). These energy profiles are

quite similiar to those in the HH channel (9, 23), but ~2 kcal/mol higher for Cs^+ and ~2 kcal/mol lower for Cl^-.

The energy profile for Cs^+ has two binding sites near the channel mouths at 12.4 Å from the midpoint. At the binding site Cs^+ binds strongly with the No. 2 CO and the adjacent NH of the strand which has its formyl end in this mouth. The center of mass distance between the ion and the CO is 3.0 Å, and that between the ion and the NH is 4.5 Å. As was our previous convention (9), in one monomer the formyl CO is numbered 0, the following CO groups are numbered sequentially, and the ethanolamine COH is numbered 16; in the other monomer the CO groups are numbered similarly from 0′ to 16′. In the HH channel the binding site is close to the No. 11 CO near the ethanolamine end. The specific CO group to which the cation binds depends on the helical structure. This CO group must have its oxygen atom oriented towards the entering cation and be located with enough space to allow the cation to get close while not being strongly repelled by neighboring groups. The binding energy at the binding site of the APDS channel is 2.9 kcal/mol higher than that in the HH channel.

As Cs^+ moves towards the midpoint from the binding site in the APDS channel, at 9.3 Å from the channel midpoint there is an energy barrier of 10.0 kcal/mol, 3.2 kcal/mol higher than the similar barrier in HH channel. Then, the energies decrease 5.6 kcal/mol from 9.3 Å to the channel midpoint.

Cs^+ interacts with both strands of APDS channel, but at most of the locations it does not interact equally well with them. This can be rationalized from the electric potential in Fig. 2 *a*. When Cs^+ approaches an APDS channel from the negative z direction, the potential from strand 1 is lower than that from strand 2 and Cs^+ stays closer to strand 1. At the binding site Cs^+ binds strongly with the No. 2 CO of strand 1 while the interaction energy with strand 2 is only about one third of that with strand 1. Because of the strong polarization due to the ion the electric potential of strand 1 is further lowered and the cross-over point for the two monomer potentials shifts to more positive z direction. The energy partitioning study shows that at ~ -9.3 Å the interaction with strand 2 becomes larger than that with strand 1. From -9.3 Å to the midpoint Cs^+ is off axis 0.5–0.8 Å and interacts more favorably with strand 2. This is qualitatively consistent with the electric potential curve in Fig. 2 *a*. At the channel midpoint ($z = 0$) Cs^+ location is off axis 0.8 Å and is symmetrical with respect to both strands. At this position Cs^+ interacts equally well with both strands. It interacts most strongly with No. 10 CO of strand 1 and No. 10′ CO of strand 2 at the same distance of 3.4 Å.

WATER-APDS INTERACTION

All ion transport processes are in aqueous solution. Fig. 4 shows a calculated stable configuration of 13 water molecules in an APDS channel. Like the HH channel, water in the APDS channel forms a single-file chain of seven to nine molecules. Each single file water molecule binds to the oxygen atom of a neighboring water molecule with one of its hydrogen atoms and to the polar groups of the channel wall with the other hydrogen atom. The water dipoles in the single-file region are pointed in the same general direction and may change their directions near the channels mouths. These features are the same as in the HH channel (23, 27, 28).

In the single-file region water molecules are off axis ~0.9 Å and the distances between neighboring water molecules are ~3.0 Å (axial separations are 2.6–2.8 Å). In the HH channel they are off axis 0.2–0.6 Å and the distances between neighboring molecules are from 2.9 to 3.3 Å (axial separations are 2.8–3.3 Å). It appears that in the APDS channel water molecules are more off axis and the average water–water distance is smaller than in HH channel. What about the water-channel interaction? In this 13–water molecule calculation the water-channel interaction energy in the APDS channel (defined as the total energy of the water-channel system minus the sum of the empty channel energy and the 13–water molecule cluster energy) is 9.5 kcal/mol higher than that for the HH channel. Water-APDS interaction is less favorable than water-HH interaction. This is one possible reason for HH being the dominant transmembrane channel isomer.

Plotting the energy profile of a single water molecule in the APDS channel, as shown in Fig. 5 (*circles*), illustrates some aspects of the water-APDS interaction. The average binding energy of a single water molecule in the APDS channel is -8 to -10 kcal/mol, which is higher than that in an HH channel (-10 to -12 kcal/mol). This is consistent with the less favorable water-APDS interaction energy in the 13–water molecule calculation. Another difference is the 3 Å pseudoperiodicity, twice as large as that in the HH channel. Comparing Figs. 4 and 5 we find that in the stable 13-molecule configuration most of the

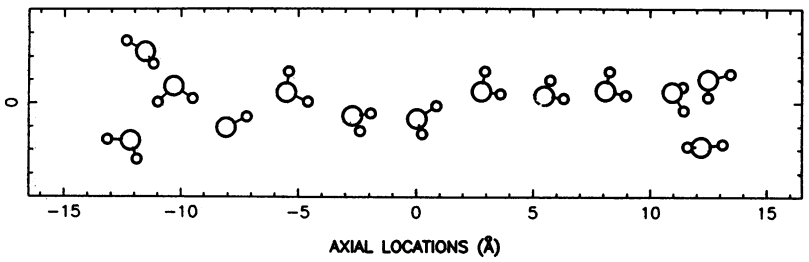

FIGURE 4 A representative water structure in an APDS channel, illustrating the dipolar orientations of the single file of water molecules. The channel groups are not shown.

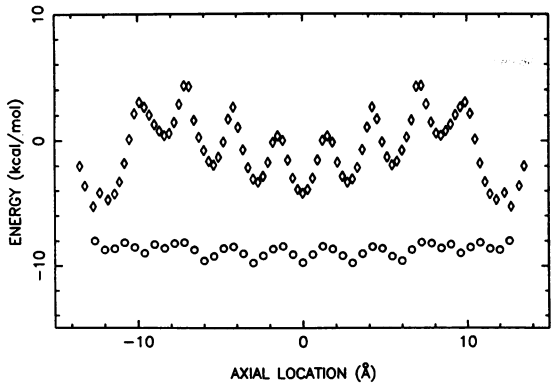

FIGURE 5 The interaction energy (*circles*) of a single water molecule in an APDS channel and the channel solvation energy (*diamonds*) for Cs^+ in an APDS channel with four water molecules. The detailed structure in the ionic solvation energy reflects the influence of the water; it differs greatly from that in the water-free channel (Fig. 3).

single-file waters are located near the energy minima of the single–water molecule energy profile. Because the water–water axial separation roughly equals the 3 Å pseudoperiodicity, when one molecule in the single file is near a saddle point, several neighboring molecules will be in the vicinity of other saddle points. This may amplify the energy barriers as the single file of water moves in the APDS channel. In the HH channel the pseudoperiodicity is 1.5 Å; water–water distances are more variable and the associated energy barriers are smaller.

Cs^+ AND WATER IN APDS CHANNEL

Rather than attempting a complete calculation including membrane and bulk water, we focus on the computationally tractable problem of analyzing a channel system with only a few water molecules. As described previously (9), with water molecules included we define channel solvation energy as the energy change in the reaction $Cs^+ \cdot (H_2O)_m + \text{Gram}(H_2O)_n = (H_2O)_m + \text{Gram}(Cs^+(H_2O)_n)$, where the first terms on both sides are the calculated cluster energies, the second term on left is the calculated energy for a water-channel system with water molecules located in the central region of the channel, and the second term on right is that for an ion-water-channel system with Cs^+ at various locations. This process involves partial dehydration (water is removed from the first hydration shell) and resolvation (the ion coordinates to gramicidin's polar moieties).

With four water molecules in the clusters ($m = 4$), representing the first hydration shell, and four water molecules in the channel ($n = 4$), two on each side of Cs^+ in the single-file region, the channel solvation energy is illustrated in Fig. 5 as diamonds. Comparison with the Cs^+ profile for the anhydrous channel in Fig. 3 shows the persistence of the binding sites near the channel mouths. The binding site is 12.7 Å from the channel midpoint and 2.2 Å off axis. Here, as in the water-free case, Cs^+ binds most strongly to the No. 2 CO group at distance of 3.1 Å. It also interacts quite favorably with the ethanolamine COH group, No. 4 CO, No. 3 NH, No. 11′ CO, and No. 13′ CO. Near the binding site there is another relative minimum (11.8 Å from the midpoint and 1.2 Å off axis) 0.5 kcal/mol higher than that of the binding site. Here Cs^+ also binds most strongly with No. 2 CO (at distance of 3.2 Å), but interacts more favorably with No. 6 CO than the ethanolamine COH group. However, with 12 water molecules in the channel this site is no longer a relative minimum. At the binding site three of the four water molecules are within 3.4 Å of the Cs^+; the fourth is located deep in the single-file region, separated from Cs^+ by one of the three first neighbor water molecules. If we start with a configuration where three water molecules are outside (farther from the channel midpoint than Cs^+) and one is inside (closer to the midpoint), all four of the water molecules bind to Cs^+ at distances from 3.1 to 3.4 Å. Unlike in the single-file region, here there is space for more water molecules to bind to the cation. Together with the No. 2 CO, at the binding site Cs^+ could be at least five coordinated. The location and structure of the binding site are similar to those in the HH channel (9, 23), but the channel solvation energy here is −5.2 kcal/mol, much higher than that in the HH channel.

As Cs^+ moves towards the channel midpoint, there is an energy barrier at 9.9 Å, 8.2 kcal/mol above the binding site. In the single file region there are also several high intermediate barriers because, as mentioned previously, the Cs^+-water and water–water axial distances are nearly equal to the pseudoperiodicity. These intermediate barriers are as large as 6.2 kcal/mol, much higher than those (<4 kcal/mol) in the HH channel (9). The energies in the single-file region vary from −4.21 kcal/mol (at 0 Å) to 4.31 kcal/mol (at 7.2 Å), ~3 kcal/mol higher on average than those in the HH channel.

In the single file region Cs^+ is 0.3–0.7 Å off the channel axis. Just as in the water free channel, the Cs^+ trajectory follows a helix of the same handedness and pitch as that of the channel helix. Because of the complicated interactions with ion and water molecules, the simple pattern of the monomer potential shown in Fig. 2 is greatly perturbed and no longer leads to cation preference for a particular strand.

At the channel midpoint the cation and water molecules interact symmetrically with both strands. The Cs^+-water distance is 3.2 Å and the neighbor water–water distance to either side of Cs^+ is 3.0 Å. Cs^+ is 0.6 Å off axis and interacts most strongly with the No. 10 COs at a distance of 3.6 Å.

To further elucidate the role water plays in the APDS channel, calculations with 12 channel waters ($n = 12$) and four cluster waters ($m = 4$) were carried out. The channel is occupied to ~13 Å from its midpoint on each side. With a total of 12 water molecules, the number of waters on either side of the ion is dependent on the ion's z position. With

Cs^+ in the mouth, two water molecules are outside and 10 are inside. As Cs^+ moves into the channel, the water partitioning becomes 3–9, 4–8, 5–7, and 6–6, sequentially. These distributions correspond to the low energy configurations for Cs^+ at particular z. Their solvation energies are shown in Fig. 6 by diamond symbols. The analogous channel solvation energy for Cs^+ in an HH channel with 12 water molecules is also illustrated (*stars*).

This energy profile in the APDS channel is similar to that of Fig. 5, with some quantitative differences. Except the small wiggle near the binding site in Fig. 5, both figures show the same number of energy maxima and minima. The structural features are also like those found in the four-water calculation. In the single file region Cs^+ is 0.4–0.8 Å off axis, water-Cs^+ distances are 3.1–3.2 Å and water–water distances are 2.9–3.0 Å.

With 12 water molecules in the APDS channel the major binding sites near the mouths are 12.7 Å from the midpoint. The channel solvation energy at this binding site is 1.0 kcal/mol higher than that in HH. The energy at the 9.3 Å peak in the APDS profile is quite large, 12.4 kcal/mol above that of the binding site; in HH this difference is only 8.8 kcal/mol. In the single-file region of APDS the energy is ~5.0 kcal/mol higher on average than that in HH. Altogether there are 15 energy barriers in HH; there are only eight in APDS due to the larger pseudoperiodicity. However, as seen in the figure, the barriers in APDS are generally higher than those in HH. All these suggest that the APDS channel should have lower cation conductance.

SUMMARY

From the energy calculations and the structural analysis discussed above, the APDS channel should have the same valence selectivity as the HH channel: cation selective. However, its self-interaction energy is higher, indicating its isolated form to be less stable. Its dimerization energy is much larger due to more intermonomer hydrogen bonds, consistent with its much longer lifetime. Its interaction energy with water is higher, implying that it is less able to act as a transmembrane channel in aqueous solution. Compared with HH, the channel solvation energy for Cs^+ is generally higher with larger barriers, suggesting a lower cation conductance.

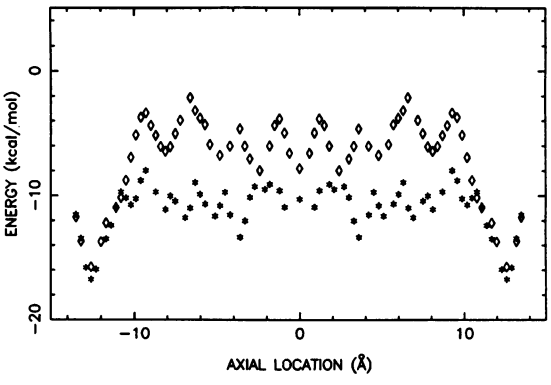

FIGURE 6. The channel solvation energy for Cs^+ in a channel with 12 water molecules. (*Diamonds*) the APDS channel; (*stars*) the HH channel. Note the higher average potential energy and the larger barriers for the APDS channel. The periodicity in the APDS channel is ~3.0 Å; that in HH is ~1.5 Å. The APDS solvation profile is not markedly different from that found with only four water molecules (Fig. 5). It differs substantially from that of the water-free case (Fig. 3).

We are very grateful to Dr. R. E. Koeppe II for providing us with his calculated APDS coordinates.

This work has been partly supported by grant GM-28643 from the National Institutes of Health and by instrumentation grants from the National Institutes of Health and the National Science Foundation. Acknowledgment is also made to the Donors of The Petroleum Research Fund, administered by the American Chemical Society, for partial support of this research.

Received for publication 4 January 1988 and in final form 9 May 1988.

REFERENCES

1. Urry, D. W. 1971. The gramicidin A transmembrane channel. *Proc. Natl. Acad. Sci. USA.* 68:672–676.
2. Urry, D. W., T. L. Trapane, and K. U. Prasad. 1983. Is the gramicidin A transmembrane channel single strand or double strand helix? A simple unequivocal determination. *Science (Wash. DC).* 221:1064–1067.
3. Durkin, J. T., O. S. Andersen, F. Heitz, Y. Trudelle, and R. E. Koeppe II. 1987. Linear gramicidins can form channels that do not have the $\beta^{6.3}$ structure. *Biophys. J.* 51:451*a*. (Abstr.)
4. Veatch, W. R., E. T. Fossel, and E. R. Blout. 1974. The conformation of gramicidin A. *Biochemistry.* 14:5249.
5. Koeppe, R. E. II, J. M. Berg, K. O. Hodgson, and L. Stryer. 1979. Gramicidin A crystals contain two cation binding sites per channel. *Nature (Lond.).* 279:723–725.
6. Wallace, B. A. 1986. The structure of gramicidin A. *Biophys. J.* 49:295–306.
7. Koeppe, R. E. II, and M. Kimura. 1984. Computer building of β-helical polypeptide model. *Biopolymers.* 23:23–38.
8. Lee, W. K., and P. C. Jordan. 1984. Molecular dynamics simulation of cation motion in water-filled gramicidinlike pores. *Biophys. J.* 46:805–819.
9. Sung, S.-S., and P. C. Jordan. 1987. Why is gramicidin valence selective? A theoretical study. *Biophys. J.* 51:661–672.
10. Schulz, G. E., and R. H. Schirmer. 1979. The Principles of Protein Structure. Springer-Verlag, New York.
11. Pething, R. 1979. Dielectric and Electronic Properties of Biological Materials. John Wiley & Sons, Chichester, UK.
12. Barnes, P., J. L. Finney, J. D. Nicholas, and J. E. Quinn. 1979. Cooperative effect in simulated water. *Nature (Lond.).* 282:459–464.
13. Shepard, A. C., Y. Beer, G. P. Klein, and L. S. Rothman. 1973. Dipole moment of water from stark measurements of H_2O, HDO, and D_2O. *J. Chem. Phys.* 59:2254–2259.
14. Neumann, D., and J. W. Moskowitz. 1968. One-electron properties of near-Hartree-Fock wavefunctions. I. Water. *J. Chem. Phys.* 49:2056–2070.
15. Eisenberg, D., and W. Kauzman. 1969. The Structure and Properties of Water. Clarendon, Oxford, UK.
16. Gowda, B. T., and S. W. Benson. 1982. Empirical potential parameters for alkali halide molecules and crystals, hydrogen halide molecules, alkali metal dimers and hydrogen and halogen molecules. *J. Phys. Chem.* 86:847–857.
17. Gellatly, B. J., J. E. Quinn, P. Barnes, and J. L. Finney. 1983. Two,

three, and four body interactions in model water interactions. *Mol. Phys.* 50:949–970.

18. Sung, S.-S., and P. C. Jordan. 1986. Structures and energetics of monovalent ion-water microclusters. *J. Chem. Phys.* 85:4045–4051.
19. Ashadi, M., R. Yamdagni, and P. Kebarle. 1970. Hydration of the halide negative ions in the gase phase. II. Comparison of hydration energies for the alkali positive and halide negative ions. *J. Phys. Chem.* 74:1475–1482.
20. Dzidic, I., and P. Kebarle. 1970. Hydration of the alkali ions in the gas phase. Enthalpies and entropies of reactions $M^+ (H_2O)_{n-1} + H_2O = M^+(H_2O)_n$. *J. Phys. Chem.* 74:1466–1474.
21. Desnoyers, J. E., and C. Jolicoeur. 1969. Modern Aspects of Electrochemistry. Vol. 5. Ch. 1. J. O. Bockris and B. E. Conway, editors. Plenum Publishing Corp., New York.
22. Sung, S.-S., and P. C. Jordan. 1987. The interaction of Cl^- with a gramicidin-like channel. *Biophys. Chem.* 27:1–6.
23. Sung, S.-S., and P. C. Jordan. 1988. A theoretical study of double ion occupancy in a gramicidin-like channel. *J. Phys. Chem.* 92:2362–2366.
24. Gear, C. W. 1971. Numerical Initial Value Problems in Ordinary Differential Equations. Prentice-Hall, Inc., Englewood Cliffs, NJ.
25. Evans, D. J., and S. Murad. 1977. Singularity free algorithm for molecular dynamics simulation of rigid polyatomics. *Mol. Phys.* 34:327–331.
26. Koeppe, R. E. II, K. O. Hodgson, and L. Stryer. 1978. Helical channel in crystals of gramicidin A and of a cesium-gramicidin A complex: an x-ray diffraction study. *J. Mol. Biol.* 121:41–54.
27. Mackay, D. J., P. H. Berens, K. R. Wilson, and A. T. Hagler. 1984. Structure and dynamics of ion transport through gramicidin A. *Biophys. J.* 46:229–248.
28. Kim, K. S., H. L. Nguyen, P. K. Swaminathan, and E. Clementi. 1985. Na^+ and K^+ ion transport through a solvated gramicidin A transmembrane channel: molecular dynamics studies using parallel processors. *J. Phys. Chem.* 89:2870–2876.